Supplementary information for:

Magnetic bacterial protein Mms6 controls morphology, crystallinity and magnetism of cobalt-doped magnetite nanoparticles *in vitro*

Johanna M Galloway[a], Atsushi Arakaki[b], Fukashi Masuda[b], Tsuyoshi Tanaka[b], Tadashi Matsunaga[b] and Sarah S Staniland*[a]

[a] School of Physics and Astronomy, University of Leeds, Leeds, LS2 9JT, UK. Fax: +44 (0) 113 3433900; Tel: +44 (0)113 3433399; E-mail: *[a]s.s.staniland@leeds.ac.uk
[b] Department of Biotechnology, Tokyo University of Agriculture and Technology, 2-24-16 Naka-cho, Koganei, Tokyo, 184-8588, Japan.

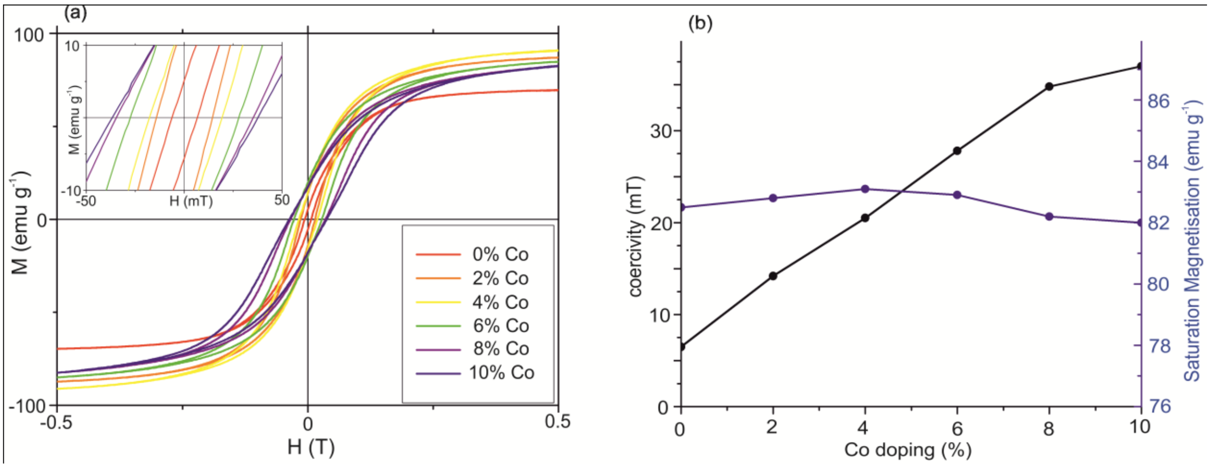

Supplementary Fig. S1. Preliminary magnetic data for POFHN method for dried particles formed in the absence of Mms6. Hysteresis loops containing an inset of a close up of the centre of plot (a) and comparison of coercivity and saturation magnetisation (b). The coercivity improves with increased levels of Co doping, but there is little variation in the saturation magnetisation. The cross over point on the comparison (b) is arbitrary as it is scale dependent. This method is unsuitable for optimisation as there is poor grain size and morphology control, and little variation in the saturation magnetisation. This lack of response may be due to a complex interplay between the various particle sizes, as well as various morphologies being present and / or cobalt not being incorporated into the MNPs formed by the POFHN method.

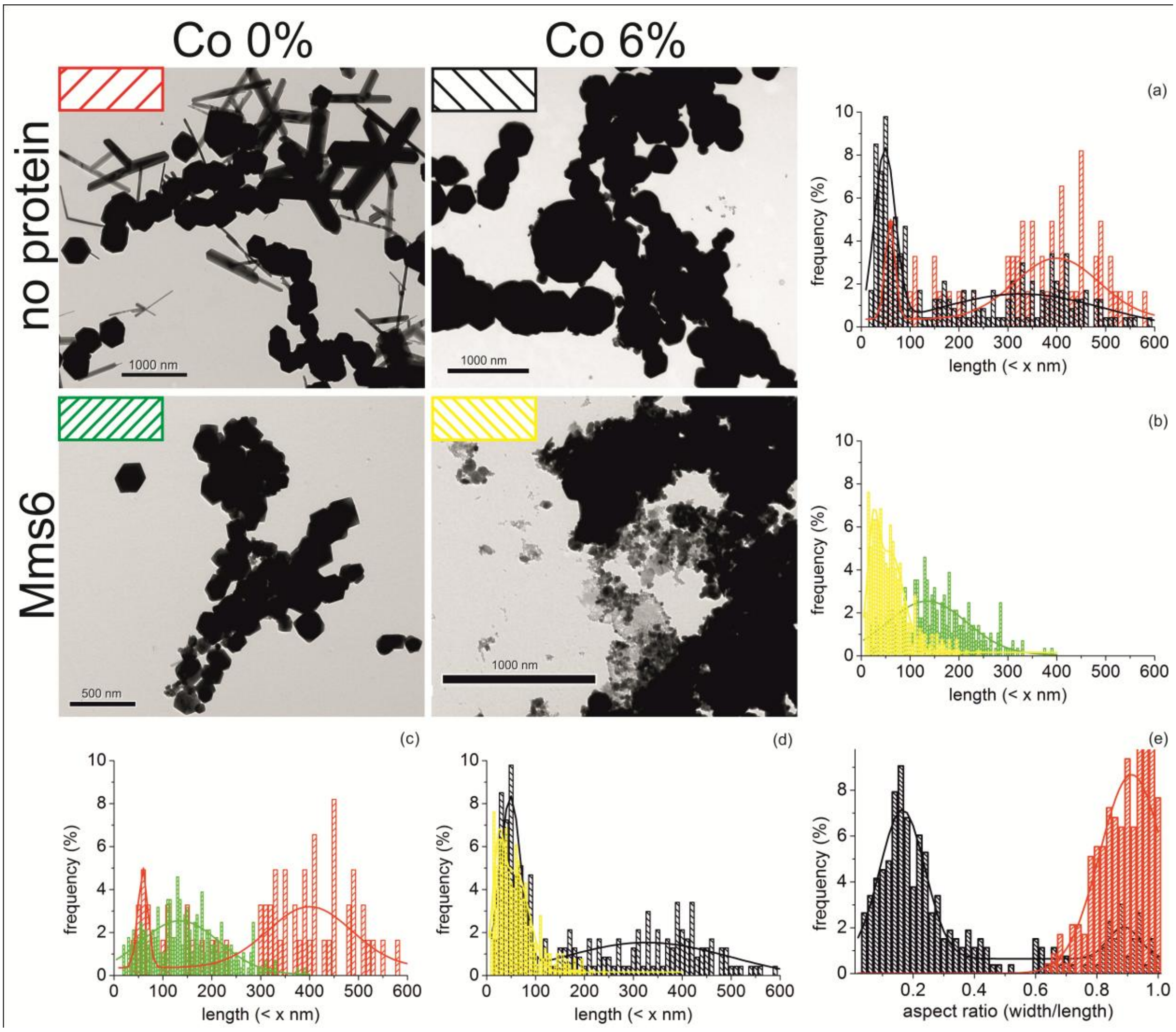

Supplementary Fig. S2. TEM images and grain size analysis for ammonia and hydrazine POFHN method. More acicular than equidimensional particles in $Fe_{no\ protein}$, with very few needle shaped particles produced when Co or Mms6 are included in the reaction. Graphs (a) to (d) compare grain size of octahedral or cubo-octahedral particles (width to length ratio > 0.5). Particles formed without protein are frequency distributed into bin size of 10 and fitted with a 2 peak Gaussian distribution, shown as red ($Fe_{no\ protein}$) and black ($Co_{no\ protein}$). Those formed with Mms6 are distributed into bin size of 5, with Fe_{Mms6} (green) fitted with a single Gaussian and Co_{Mms6} (yellow) fitted with a double Gaussian. Graph (e) compares the roundness (width to length ratio) of $Fe_{no\ protein}$ (red – double Gaussian) and with $Co_{no\ protein}$ (black – single Gaussian).

Supplementary Fig. S2 shows that the POFHN method (both with and without cobalt, but no protein) has a large variation in the size of particles formed in the absence of protein (between ~10 and 700 nm) and two distinct species could be seen with peaks around 50 and 400 nm. There were many more acicular particles than equidimensional particles observed in the $Fe_{no\ protein}$ MNPs, as such only ~60 of the 265 MNPs measured were included in the grain size analysis. The addition of Mms6 and / or the doping of Co dramatically reduced the occurrence of needle shaped particles. This shape anisotropy may dominate the magnetic behaviour over the alteration due to increasing levels of Co doping. The addition of Mms6 also formed a much higher proportion of cubo-octahedral MNPs. The biomineralising protein also reduced the maximum particle size to ~390 nm for Fe_{Mms6} and ~240 nm for Co_{Mms6} (see Table 1). Markedly, we see that the peak centre reduces to 135 nm and 24 nm respectively with the addition of protein.

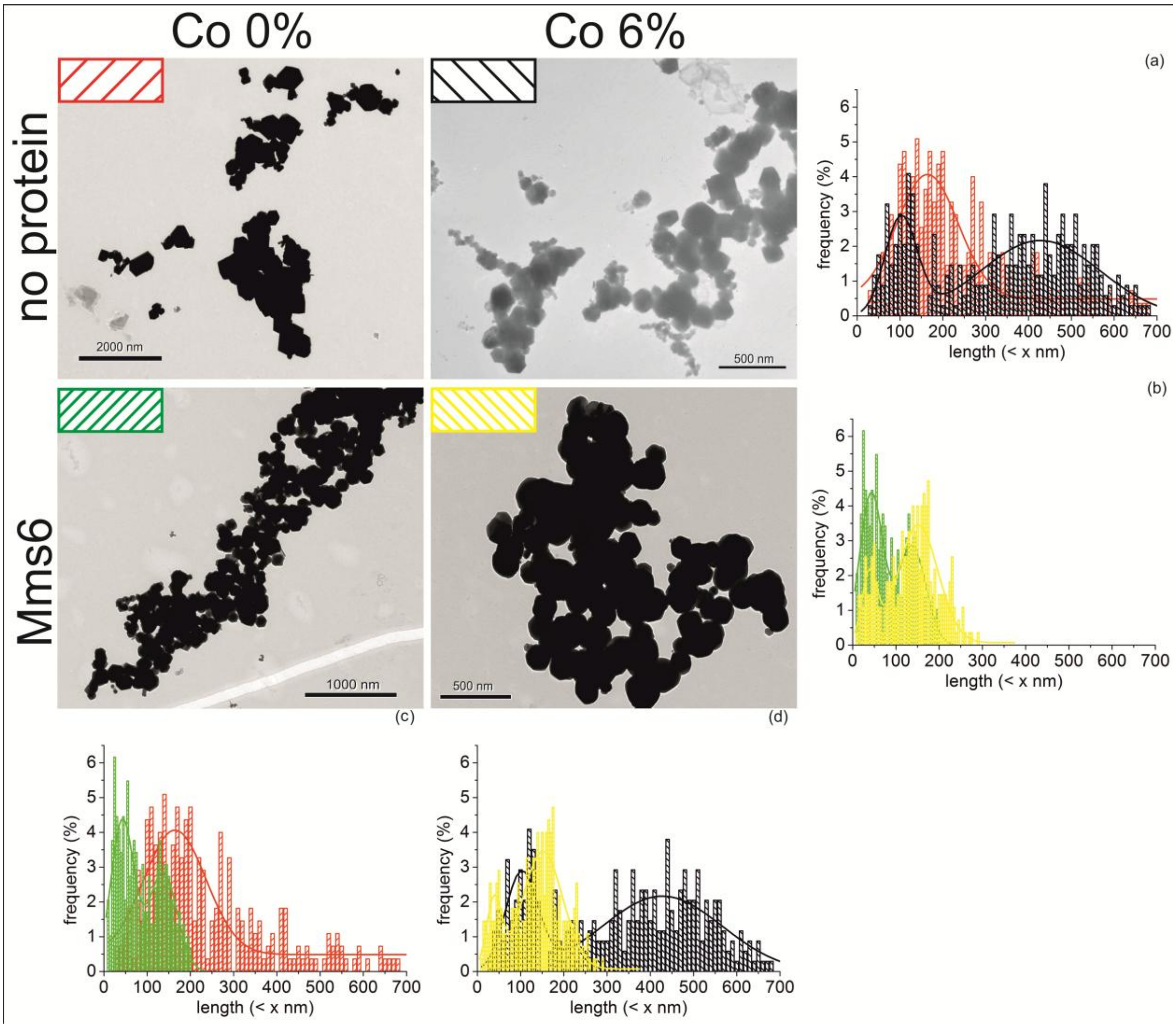

Supplementary Fig. S3. TEM images and grain size analysis for potassium hydroxide POFHK method. Graphs (a) – (d) compare grain size of equidimensional particles (width to length ratio > 0.5). Particles formed without protein are frequency distributed into bin size of 10 and fitted with a single peak Gaussian distribution, shown as red ($\mathrm{Fe}_{\text{no protein}}$) and 2 peak Gaussian fit, shown as black ($\mathrm{Co}_{\text{no protein}}$). Those formed with Mms6 are distributed into bin size of 5, with $\mathrm{Fe}_{\text{Mms6}}$ (green) and $\mathrm{Co}_{\text{Mms6}}$ (yellow) fitted with 2 peak Gaussian distributions. There are very few acicular particles and the size range of the MNPs formed without protein is large, ranging from ~20 nm to ~730 nm for $\mathrm{Fe}_{\text{no protein}}$ and to ~820 nm for $\mathrm{Co}_{\text{no protein}}$. Here, the inclusion of 6% cobalt into the magnetite particles also appears to increase the proportion of larger MNPs, whether or not Mms6 is added. The use of Mms6 during particle formation again appears to significantly suppress the maximum grain size, to ~290 nm for $\mathrm{Co}_{\text{Mms6}}$ and ~200 nm for $\mathrm{Fe}_{\text{Mms6}}$ (see Table 1). The numbers of acicular grains formed by RTCP make up less than 10% of the crystal morphologies present in all cases (data not shown), but was significantly less for the his_6Mms6 and Mms6 samples, again showing that the protein suppresses the formation of needle shaped crystals.

method	Co in initial solution [%]	Co in particles [%]	Error [±]	Difference
POFHK	0	0		
	2	4.0	0.6	200%
	6	10.6	1.7	177%
	10	15.7	2.5	157%
	15	20.0	3.3	133%
POFHN	0	0		
	2	3.9	0.6	195%
	4	8.0	1.3	200%
	6	9.6	1.5	160%
	8	14.3	2.3	179%
	10	17.1	2.7	171%
RTCP	0	0		
	6	4.8	0.8	80%

Supplementary Table S1. ICP-OES data table of abundance of iron and cobalt ions in the dissolved MNPs. All methods shown did not use the biomineralising protein and percentages are expressed as proportion of metal ions. This shows that both POFH methods preferentially incorporate Co^{2+} over Fe^{2+} into MNPs from the salt solutions. This rules out differential Co inclusion into MNPs causing the lack of variation in saturation magnetisation (see Supplementary Fig. S2). The RTCP method appears to slightly preferentially incorporate Fe^{2+} over Co^{2+}, so an increase in Co^{2+} levels in the ion solution could further improve coercivity for this method of MNP synthesis.

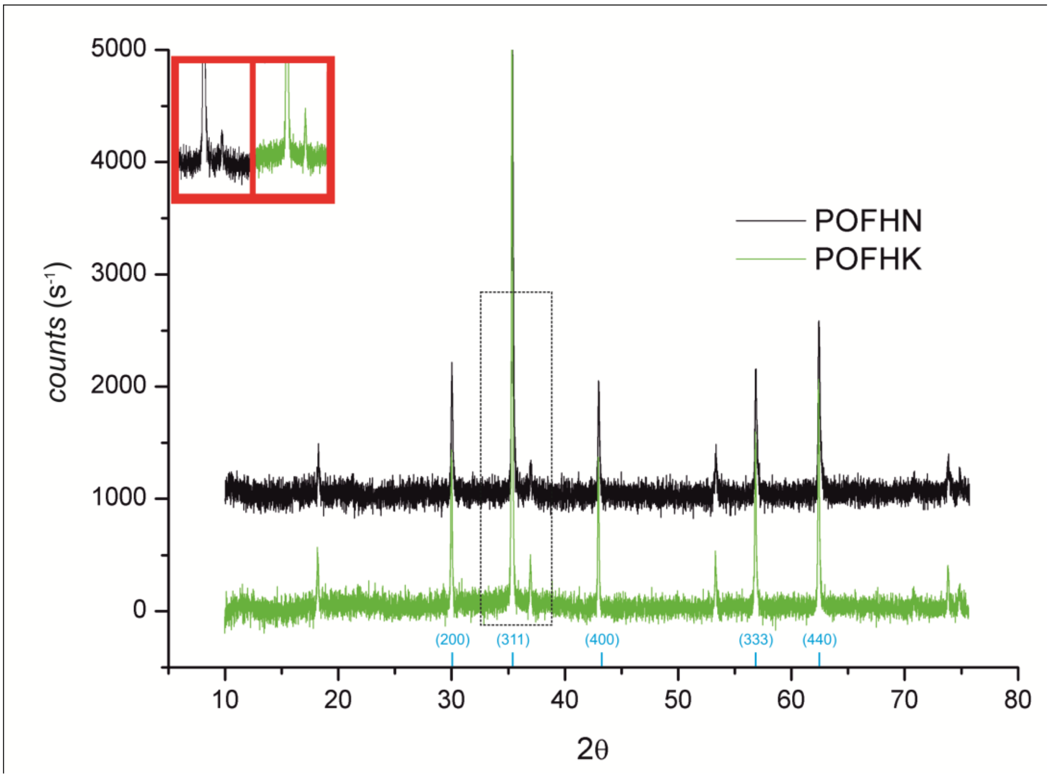

Supplementary Fig. S4. Powder XRD analysis of POFHN and POFHK methods show the materials produced are all magnetite species with no impurities. (311) peak at $2\theta = 35.4°$ from both are in same area. The low intensity suggests poor crystallinity of the MNPs, and the sharpness of the peaks reflects the large grain size. This correlates well with the data shown above including the grain sizes from TEM . Also, as the magnetic saturation of POFHN MNPs varies little with changing levels of Co, which could be due to poor crystallinity This is supported by the ICP-OES data (the MNPs do incorporate Co from the salt solutions) and the grain size data shows the majority of MNPs formed are well above the SD size threshold.

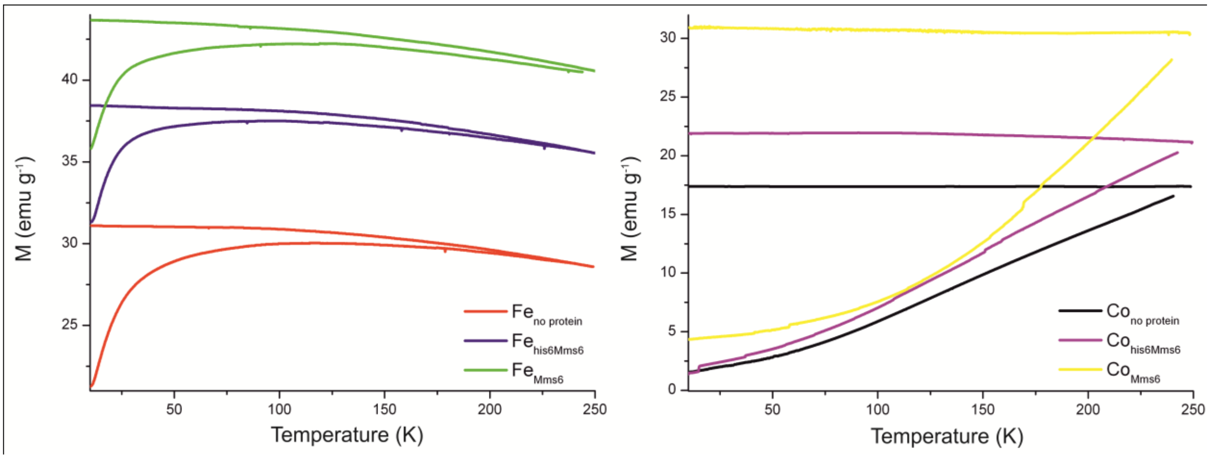

Supplementary Fig. S5. VSM of field cooled (FC, top line) and zero field cooled (ZFC, lower line) moment vs temperature measurements. Samples are cooled in a zero applied field to 10 K then warmed at 1 K minute^{-1} in a 0.1 T applied field to 250 K for ZFC. For FC measurements the MNPs are then cooled at the same rate, in the same field from 250 K to 10 K. Left - undoped magnetite MNPs, right - 6% Co doped MNPs. Magnetite MNPs have a blocking temperature between 100-200 K. The greater coercivity of Co doped MNPs shows more gradual unblocking of ZFC moments as the particles are heated towards a much higher blocking temperature. It is not possible to fully resolve a precise blocking temperature for the MNPs due to the range in particle sizes (see Table 1 for FWHM of particles), but this range is consistent with magnetite MNPs of these sizes (e.g. see Goya *et al.*[1]). The Co doped MNPs have much higher blocking temperature, $T_B > 250$ K (probably around room temperature). Further investigation of this would require magnetometry at temperatures well above the stability range for the VSM used in this study. There is no evidence of the Verwey Transition which was expected. The Verwey Transition appears as a sharp drop in magnetisation at 120 K for bulk magnetite, and is due to recrystallisation of stiochiometric, pure magnetite from a cubic to a monoclinic structure at low temperatures.[2-3] As SP magnetite is able to completely suppress this,[4-6] and our magnetite MNPs are below the single domain size threshold for magnetite (Fe_{Mms6} = 21.9 nm), they should not show the Verwey Transition. Also, impurities can significantly depress or obscure this transition[3, 6-8], thus the cobalt doping may act as an impurity and therefore suppress the Verwey Transition in the 6% Co doped MNPs above the SD size threshold.

References

1. G. F. Goya, T. S. Berquo, F. C. Fonseca and M. P. Morales, *J. Appl. Phys.*, 2003, **94**, 3520-3528.
2. E. J. Verwey, P. W. Haayman and F. C. Romeijn, *J. Chem. Phys.*, 1947, **15**, 181-187.
3. F. Walz, *J. Phys. Condens. Matter*, 2002, **14**, R285.
4. B. M. Moskowitz, R. B. Frankel and D. A. Bazylinski, *Earth Planet. Sci. Lett.*, 1993, **120**, 283-300.
5. B. M. Moskowitz, R. B. Frankel, D. A. Bazylinski, H. W. Jannasch and D. R. Lovley, *Geophys. Res. Lett.*, 1989, **16**, 655-688.
6. O. Ozdemir, D. J. Dunlop and B. M. Moskowitz, *Geophys. Res. Lett.*, 1993, **20**, 1671-1674.
7. R. Aragón, *Phys. Rev. B*, 1992, **46**, 5328.
8. R. Aragón, D. J. Buttrey, J. P. Shepherd and J. M. Honig, *Phys. Rev. B*, 1985, **31**, 430.